Available online at www.sciencedirect.com
SCIENCE DIRECT®
International Journal of Thermal Sciences 42 (2003) 513–521
International Journal of Thermal Sciences
www.elsevier.com/locate/ijts

Analysis of entropy generation inside concentric cylindrical annuli with relative rotation

Shohel Mahmud *, Roydon Andrew Fraser

Department of Mechanical Engineering, University of Waterloo, 200 University Avenue West, Waterloo, ON, Canada N2L 3G1

Received 27 November 2001; accepted 20 June 2002

Abstract

The present article investigates analytically the First and Second Laws (of Thermodynamics) characteristics of fluid flow and heat transfer inside a cylindrical annulus. A relative rotational motion presents between the inner and the outer cylinders which induces the flow. Two different cases are considered: (a) both cylinders are isothermal and kept at different temperatures and (b) the outer cylinder is isoflux and the inner is isothermal. Governing equations in cylindrical coordinates are simplified and solved to obtain analytical expressions for dimensionless entropy generation number (N_S), irreversibility distribution ratio (Φ), and the Bejan number (Be) as a function of flow governing and geometric parameters. Spatial distribution of velocity and temperature, volumetric and average entropy generation rate, and heat transfer irreversibility are presented graphically. The effect of velocity ratio (λ), the group parameter (Br/Ω), and the Brinkman number (Br) on the above parameters are tested.

Keywords: Bejan number; Entropy generation number; Irreversibility distribution ratio

1. Introduction

Flow induced by a relative rotating motion or axial movement between cylinders in a concentric arrangement has many significant engineering applications. In addition to heat transfer situations, the resulting flow is particularly applicable to rotating electrical machines, swirl nozzles, rotating disks, standard commercial rheometers, and other chemical and mechanical mixing equipment (see Maron and Cohen [1]). Since the pioneering work of Taylor [2], numerous analytical and experimental works have been performed to predict flow, and thermal fields, stability, heat/mass transfer characteristics, etc., inside the concentric annular space. For one fixed and one rotating cylinder, Astill [3] and Andereck et al. [4] presented a developing flow with different flow regimes inside a concentric cylindrical annulus. Heat transfer studies have been primarily stimulated by cooling problems in the design of electric motors of high power density (see Maron and Cohen [1]). Most experimental investigations focused on the measurements of heat transfer coefficients in a rotating inner cylinder system with and without axial flow. Bjorklund and Kaye [5] proposed a correlation for heat transfer measurement based on their experimental data for zero axial flow. Later work of Tachibana et al. [6] showed excellent agreement with the correlation of Bjorklund and Kaye [5]. Aoki et al. [7] predicted theoretically the overall heat transfer coefficients limited to a small gap widths for a fluid having Prandtl number equal to 1. Effect of natural convection was studied by Leonardi et al. [8] for a finite annular gap with differentially heated walls. El-Shaarawi and Sarhan [9], Gardiner and Sabersky [10], and Gasley [11] have significant contributions related to above-mentioned researches. The foregoing discussions are some of the extensive research efforts concerning flow and heat transfer between rotating surfaces. For a comprehensive review, see the paper by Dorfman [12] or Childs and Long [13].

The foregoing discussions are a small part of wide research efforts related to flow and thermal problems inside annular gap with rotating or axially moving cylinder. Although these works have covered a wide variety problems involving concentric cylinders, these problems have been restricted, in thermodynamic point of view, to only the First Law (of Thermodynamics) analyses. The contemporary trend in the field

* Corresponding author.
E-mail addresses: smahmud@engmail.uwaterloo.ca (S. Mahmud), rafraser@engmail.uwaterloo.ca (R.A. Fraser).

1290-0729/02/$ – see front matter
doi:10.1016/S1290-0729(02)00051-0

Nomenclature

Be	Bejan number, $= N_R/N_S$
Br	Brinkman number, $= Ec \times Pr$
C_n	integration constants, $n = 1, 2, \ldots$
C_p	specific heat at constant pressure . $kJ{\cdot}kg^{-1}{\cdot}K^{-1}$
e	exponential (2.718281)
Ec	Eckert number, $= (\omega_0.r_0)^2/(C_p.\Delta T)$
k	thermal conductivity of fluid ..... $W{\cdot}m^{-1}{\cdot}K^{-1}$
K	argument of Lambert function
N_F	entropy generation number; fluid friction
N_R	entropy generation number; radial
N_S	entropy generation number; total
P	pressure ..... Pa
Pr	Prandtl number, $= \mu.C_p/k$
q	constant heat flux at wall ..... $W{\cdot}m^{-2}$
r	radial distance ..... m
R	dimensionless radial distance, $= r/r_0$
S_G	entropy generation rate ..... $W{\cdot}m^{-3}K^{-1}$
T	temperature ..... °C
u	tangential velocity ..... $m{\cdot}s^{-1}$
U	dimensionless tangential velocity, $= u/(\omega_0.r_0)$

Greek symbols

α	thermal diffusivity ..... $m^2{\cdot}s^{-1}$
Γ_n	constants, $n = 1, 2, \ldots$
μ	dynamic viscosity ..... Pa·s
ρ	density of the fluid ..... $kg{\cdot}m^{-3}$
λ	velocity ratio, $= \omega_1.r_1/(\omega_0.r_0)$
ω	angular velocity ..... $rad{\cdot}s^{-1}$
Π	radius ratio, $= r_1/r_0$
Φ	irreversibility distribution ratio, $= N_F/N_R$
Θ	dimensionless temperature, $= (T - T_0)/\Delta T$
Ω	dimensionless temperature difference, $= \Delta T/T_0$
$\forall$	volume of the annular gap ..... m^3

Subscript and superscript

0	value at the inner cylinder
1	value at the outer cylinder
C	critical value
o	average value
T	for isothermal boundary condition
q	for isoflux boundary condition

of heat transfer and thermal design is to perform a Second Law (of Thermodynamics) analysis and its design-related concept of entropy generation and its minimization (Bejan [14]). This new trend is important and, at the same time, necessary, if the heat transfer community is to contribute to a viable engineering solution to the energy problems.

Entropy generation is associated with thermodynamic irreversibilities, which is common in all types of heat transfer processes. Different sources are responsible for the generation of entropy, for example, heat transfer down a temperature gradient, viscous effects, etc. Bejan [15] has focused on the different mechanisms behind entropy generation in applied thermal engineering. Generation of entropy destroys the available work of a system. Therefore, it makes good engineering sense to focus on irreversibilities (see Bejan [14,15]) of heat transfer and fluid flow processes and try to understand the function of related entropy generation mechanisms. Bejan [16] presented the Second Law aspect of heat transfer using different forced convection problem examples. Bejan [16] introduced the concept of entropy generation number, irreversibility distribution ratio, and presented spatial distribution profiles of entropy generation for the example problems. Since then, numerous investigations have been performed to determine the entropy generation and irreversibility profiles for different geometric configurations, flow situations, and thermal boundary conditions. Most of the works are numerical calculations due to the nonlinear nature of flow the governing equations. Very few of these works consider an analytical approach to a solution. For a concentric cylindrical annulus, Yilbas [17] presented an entropy analysis with a rotating outer cylinder and a differentially heated isothermal boundary condition. Yilbas [17] assumes a linear velocity profile and neglects the contribution of fluid friction irreversibility to entropy generation. For other geometries, Second Law analyses as well as entropy generation profiles are available in the references by Drost and Zaworski [18] and Bejan [15,16].

In this paper, the governing equations in cylindrical coordinates are simplified and solved using both isothermal and isoflux boundary conditions assuming a relative angular rotation is present between the cylinders in a concentric arrangement. Subsequently, expressions for dimensionless entropy generation number, irreversibility distribution ratio, and Bejan number are derived.

2. Physical model and derivation

2.1. First Law analysis

Consider the steady flow maintained between two concentric cylinders, shown in Fig. 1, by a steady angular velocity of one or both cylinders. Let the inner and outer

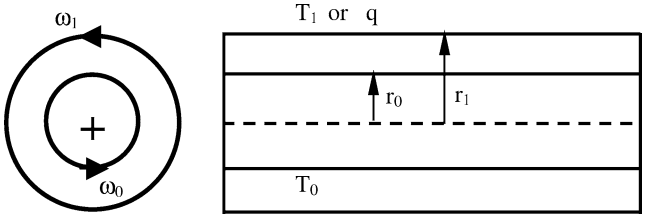

Fig. 1. Schematic diagram of the problem under consideration.

cylinders have radii r_0 and r_1, respectively. Steady angular velocities are denoted by ω_0 and ω_1 for the inner and the outer cylinders. Consider no relative axial movement between the cylinders. Neglecting the radial velocity component compared to the tangential component of the velocity, the simplified momentum equation in cylindrical coordinates is

$$\frac{\partial^2 u_\theta}{\partial r^2} + \frac{1}{r}\frac{\partial u_\theta}{\partial r} - \frac{u_\theta}{r^2} = 0 \tag{1}$$

where u_θ is the tangential velocity component. Neglecting the convection term, the energy equation becomes

$$\frac{k}{r}\frac{\partial}{\partial r}\left(r\frac{\partial T}{\partial r}\right) = -\mu\left(\frac{\partial u_\theta}{\partial r} - \frac{u_\theta}{r}\right)^2 \tag{2}$$

subjected to the following boundary conditions

$$\begin{aligned} &\text{At } r = r_0 : u_\theta = u_0 = r_0\omega_0 \text{ and } T = T_0 \\ &\text{At } r = r_1 : u_\theta = u_1 = r_1\omega_1 \text{ and } T = T_1 \text{ or } \frac{\partial T}{\partial r} = \frac{q}{k} \end{aligned} \tag{3}$$

Integrating Eq. (1) with respect to r, the solution to the momentum equation is

$$u_\theta = C_1 r + \frac{C_2}{r} \tag{4}$$

where C_1 and C_2 are two constants of integration. Applying boundary conditions described in Eq. (3), the tangential velocity u_θ takes the following form:

$$u = u_\theta = r_0\omega_0\frac{r_1/r - r/r_1}{r_1/r_0 - r_0/r_1} + r_1\omega_1\frac{r/r_0 - r_0/r}{r_1/r_0 - r_0/r_1} \tag{5}$$

In subsequent calculations, u is used in place of u_θ as tangential velocity. Expressing the ratio r_1/r_0 as Π and u_1/u_0 as λ, the dimensionless form of Eq. (5) is

$$\begin{aligned} U &= \frac{1}{\Pi^2 - 1}\left(\frac{\Pi^2 - R^2}{R}\right) + \frac{\Pi\lambda}{\Pi^2 - 1}\left(\frac{R^2 - 1}{R}\right) \\ &= \Gamma_1\left(\frac{\Pi^2 - R^2}{R}\right) + \Gamma_2\left(\frac{R^2 - 1}{R}\right) \end{aligned} \tag{6}$$

where R is the dimensionless radial distance which is equal to r/r_0. Tangential velocity u is made dimensionless dividing by $\omega_0 r_0$. The constants Γ_1 and Γ_2 are equal to $1/(\Pi^2 - 1)$ and $\Pi\lambda/(\Pi^2 - 1)$, respectively. In the above expression of velocity, constraints for different parameters are $1 \leqslant R \leqslant \infty$, $1 < \Pi \leqslant \infty$, and $-\infty \leqslant \lambda \leqslant +\infty$. For positive λ, both cylinders rotate in the same direction and for negative λ, they rotate in the opposite directions. For a stationary outer cylinder or very large rotation of the inner cylinder, the second part of Eq. (6) disappears. Before solving the energy equation (Eq. (2)) it is put into the dimensionless form. Velocity u is scaled with $\omega_0 r_0$, radial distance r is scaled with r_0, and dimensionless temperature Θ can be expressed as $(T - T_0)/\Delta T$ where T_0 is the reference temperature and ΔT is the reference temperature difference. The dimensionless form of Eq. (2) is

$$\frac{1}{R}\frac{\partial}{\partial R}\left(R\frac{\partial \Theta}{\partial R}\right) = -Ec\,Pr\left(\frac{\partial U}{\partial R} - \frac{U}{R}\right)^2 \tag{7}$$

where Ec is the Eckert number and Pr is the Prandtl number. Putting the expression for velocity U into Eq. (7) and integrating, the solution to Eq. (7) for dimensionless temperature is

$$\begin{aligned} \Theta &= C_3 + C_4\ln(R) - \frac{(\Pi - \lambda)^2}{(\Pi^2 - 1)}\frac{Ec\,Pr}{R^2} \\ &= C_3 + C_4\ln(R) - \Gamma_3\frac{Ec\,Pr}{R^2} \end{aligned} \tag{8}$$

In the above expression, C_3 and C_4 are constants of integration which depend on the boundary conditions. Γ_3 is a constant and equal to $(\Pi - \lambda)^2/(\Pi^2 - 1)$. For the isothermal boundary condition, $\Theta = 0$ at $R = 1$ and $\Theta = 1$ at $R = \Pi$. Using these values, non-dimensional temperature distribution for the isothermal boundary condition becomes

$$\Theta_T = \Gamma_3 Ec\,Pr\left(1 - \frac{1}{R^2}\right)\left[1 - \frac{\ln(R)}{\ln(\Pi)}\right] + \frac{\ln(R)}{\ln(\Pi)} \tag{9}$$

For the isoflux boundary condition, a constant heat flux q is applied to the outer cylinder, but the temperature at the inner cylinder is kept constant as isothermal case. For this particular case, $\Theta = 0$ at $R = 1$ and $\partial\Theta/\partial R = 1$ at $R = \Pi$. Using these values, non-dimensional temperature distribution for the isoflux boundary condition becomes

$$\Theta_q = \Gamma_3 Ec\,Pr\left[1 - \frac{1}{R^2} - \frac{2\ln(R)}{\Pi^2}\right] + \Pi\ln(R) \tag{10}$$

2.2. Second Law analysis

The foundations of our knowledge of entropy production goes back to Clausius and Kelvin's studies on the irreversible aspects of the Second Law of Thermodynamics. Since then the theories based on these foundations have rapidly developed. However, the entropy production resulting from temperature differences has remained untreated by classical thermodynamics thus motivating many researchers to conduct analysis of fundamental and applied engineering problems based on Second Law analyses. Review of such analyses is beyond the scope of this paper; for a comprehensive review, see Bejan [15]. Based on the Second Law of thermodynamics and assumptions already made, the local volumetric rate of entropy generation, S_G ($\mathrm{W{\cdot}m^{-3}{\cdot}K^{-1}}$), in cylindrical coordinates is shown in the following equation (for detail derivation see Bejan [15])

$$S_G = \frac{k}{T_0^2}\left(\frac{\partial T}{\partial r}\right)^2 + \frac{\mu}{T_0}\left[r\frac{\partial}{\partial r}\left(\frac{u}{r}\right)\right]^2 \tag{11}$$

The above form of entropy generation shows that the irreversibility is due to two effects, a conductive (k) effect and a viscous (μ) effect. Entropy generation rate (S_G) is positive and finite as long as temperature and/or velocity gradients are present in the medium. According to Bejan [14], the dimensionless form of S_G is the entropy generation number (N_S) and which is, by definition, equal to the ratio of actual entropy generation rate (S_G) to a characteristic

entropy transfer rate ($S_{G,C}$). According to Bejan [14,16] the characteristic entropy transfer rate is

$$S_{G,C} = \left[\frac{q^2}{kT_0^2}\right]_{\text{Isothermal}} \quad \text{or} \quad \left[\frac{k(\Delta T)^2}{r_0^2 T_0^2}\right]_{\text{Isoflux}} \tag{12}$$

The first square bracketed term is used for isoflux boundary condition and the second square bracketed term is used for isothermal boundary condition. Using the same parameters, which are already used for scaling purpose, the dimensionless form of Eq. (11) is

$$N_S = \left(\frac{\partial \Theta}{\partial R}\right)^2 + \frac{Ec\,Pr}{\Omega}\left[R\frac{\partial}{\partial R}\left(\frac{U}{R}\right)\right]^2 = N_R + N_F \tag{13}$$

In the above equation, Ω is the dimensionless temperature difference, which is equal to $\Delta T/T_0$. On the right-hand side of Eq. (13), the first term ($= N_R$) accounts for entropy generation due to heat transfer in radial direction and the second term ($= N_F$) is the fluid friction contribution to entropy generation. Combining Eqs. (6), (9), and (13), the entropy generation number (N_{ST}) for the isothermal boundary condition is

$$\begin{aligned} N_{ST} = {} & \left[\frac{2Br\Gamma_3}{R^3}\left\{1 - \frac{\ln(R)}{\ln(\Pi)}\right\}\right. \\ & \left. - \frac{Br\Gamma_3}{R\ln(\Pi)}\left(1 - \frac{1}{R^2}\right) + \frac{1}{R\ln(\Pi)}\right]^2 \\ & + \frac{4Br}{\Omega}\left[\frac{\Gamma_3\Pi^2 - \Gamma_2}{R^2}\right]^2 \end{aligned} \tag{14}$$

Combining Eqs. (6), (10), and (13), entropy generation number (N_{Sq}) for the isoflux boundary condition is

$$\begin{aligned} N_{Sq} = {} & \left[\frac{2Br\Gamma_3}{R}\left(\frac{1}{R^2} - \frac{1}{\Pi^2}\right) + \frac{\Pi}{R}\right]^2 \\ & + \frac{4Br}{\Omega}\left[\frac{\Gamma_1\Pi^2 - \Gamma_2}{R^2}\right]^2 \end{aligned} \tag{15}$$

In Eqs. (14) and (15), *Br* is the Brinkman number, which is the product of the Eckert (*Ec*) and Prandtl number (*Pr*). The Brinkman number determines the relative importance between dissipation effects and fluid conduction effects (see White [19] for details). For each expression, the first square bracketed term at the right-hand side represents heat transfer contribution and the second square bracketed term is the fluid friction contribution to entropy generation. Note that, for both isothermal and isoflux boundary conditions, fluid friction contribution to the entropy generation are same. Because flow and thermal fields are not coupled like buoyancy flow and velocity field is independent of temperature field.

2.3. Fluid friction versus heat transfer irreversibility

Entropy generates in a process or system due to the presence of irreversibility (see Bejan [14,15]). In convection problems both fluid friction and heat transfer have contributions to the rate of entropy generation. Expression of entropy generation number (N_S) is good for generating spatial entropy profile, but it fails to give any idea of whether fluid friction or heat transfer is the dominating entropy generation mechanism. According to Bejan [14], the irreversibility distribution ratio (Φ) takes care the above problem and which is equal to the ratio of entropy generation due to fluid friction (N_F) to heat transfer (N_R). Heat transfer dominates for $0 \leqslant \Phi < 1$ and fluid friction dominates when $\Phi > 1$. For $\Phi = 1$, both heat transfer and fluid friction have the same contribution for generating entropy. In many engineering designs and optimization problems (see Bejan [21]), the contribution of heat transfer entropy on overall entropy generation rate is needed. As an alternative irreversibility distribution parameter, Paoletti et al. [20] defines the Bejan number (*Be*) which is the ratio of entropy generation due to heat transfer to the total entropy generation. Mathematically Bejan number is

$$Be = \frac{N_R}{N_R + N_F} = \frac{1}{1 + \Phi} \tag{16}$$

The Bejan number ranges from 0 to 1. Accordingly, $Be = 1$ is the limit at which the heat transfer irreversibility dominates, while $Be = 0$ is the opposite limit at which the irreversibility is dominated by fluid friction effect, and $Be = 1/2$ is the case in which the heat transfer and fluid friction entropy generation rates are equal. Using Eqs. (14) and (16) and after avoiding detail mathematical operation; the Bejan number for isothermal boundary condition becomes

$$\begin{aligned} Be_T = {} & \left[Br\Gamma_3\frac{\{2\ln(\Pi/R) - R^2 + R^2/(Br\Gamma_3) + 1\}}{\{R^2\ln(\Pi)\}}\right]^2 \\ & \times \left\{\left[Br\Gamma_3\frac{\{2\ln(\Pi/R) - R^2 + R^2/(Br\Gamma_3) + 1\}}{\{R^2\ln(\Pi)\}}\right]^2\right. \\ & \left. + \frac{4Br}{\Omega R^2}\left(\Gamma_1\Pi^2 - \Gamma_2\right)^2\right\}^{-1} \end{aligned} \tag{17}$$

Using Eqs. (15) and (16), the Bejan number for isoflux boundary condition becomes

$$\begin{aligned} Be_q = {} & \left[\Pi + 2Br\Gamma_3\frac{(\Pi^2 - R^2)}{R^2\Pi^2}\right]^2 \\ & \times \left\{\left[\Pi + 2Br\Gamma_3\frac{(\Pi^2 - R^2)}{R^2\Pi^2}\right]^2\right. \\ & \left. + \frac{4Br}{\Omega R^2}\left(\Gamma_1\Pi^2 - \Gamma_2\right)^2\right\}^{-1} \end{aligned} \tag{18}$$

3. Results and discussions

In many practical situations, one of the two cylinders in the concentric orientation is kept fixed ($\lambda = 0$). This special case is presented graphically in Fig. 2 where dimensionless velocity profiles are plotted as a function of radial distance

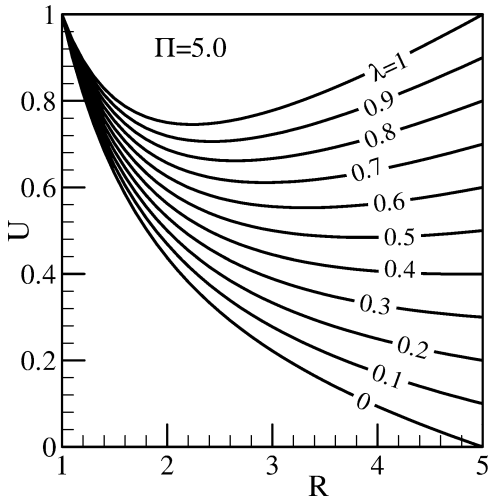

Fig. 2. Velocity profiles at different λ.

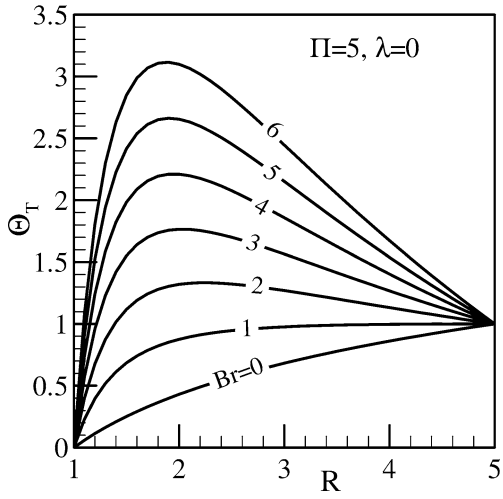

Fig. 3. Temperature distribution for the isothermal boundary condition.

for radius ratio $\Pi = 5.0$ and different velocity ratios (λ). As long as the gap between the cylinders remains small ($\Pi \approx 1$) relative to their radii, the velocity profile between the cylinders approaches the idealized linear shear flow profile (see Leal [22]). At higher Π, velocity profiles become non-linear due to the simultaneous contributions of the R and $1/R$ terms in Eq. (6). Velocity decreases along the radial direction and shows a minimum value at the outer cylinder up to $\lambda \approx 0.3846$ which can be determined from the following relation

$$\lambda = \lambda_C = \frac{2\Pi}{1+\Pi^2} \tag{19}$$

The above relation actually determines the value of λ ($= \lambda_C$) at which velocity gradient ($\partial U/\partial R$) is zero at the outer cylinder for a particular value of radius ratio (Π). For $\lambda_C < \lambda \leqslant 1$, minimum velocity occurs inside the annular gap and the radial location of the minimum velocity can be determined from the following relation

$$R_{U_{\min}} = \sqrt{\frac{\Pi(\Pi-\lambda)}{\Pi\lambda - 1}} \tag{20}$$

The above relation is important, because at this radial position, fluid friction contribution to the rate of entropy generation is zero due to the zero velocity gradient ($\partial U/\partial R$).

At the first part of this section, discussion is restricted to the isothermal case and the isoflux case will be discussed later. Fig. 3 shows the dimensionless temperature profiles as a function of radial distance for $\lambda = 0$ and $\Pi = 5.0$ at different Br ($= Ec \times Pr$). Temperature is equal to 0 and 1 at the inner and the outer cylinder, respectively. For $Br > 1$, temperature rise inside the fluid is significant due to the dissipation effect. A marked peak value of temperature occurs inside the annular space, which is higher in magnitude than the hot wall temperature. The wall heat flux actually is into the outer cylinder even though the imposed temperature difference would initially have been considered to cause wall heat flux to be out of the outer cylinder. The peak location of temperature is also important, because at this position entropy generation due to radial temperature gradient ($\partial T/\partial R$) is zero. For any value of λ, Π, and Br, the radial location for the peak value of temperature can be obtained from the following expression

$$R_{\Theta_{\max}} = \Pi \exp\left[-\frac{1}{2}\,\text{LambertW}\left\{\frac{(\Gamma_3 Br - 1)\Pi^2 e}{\Gamma_3 Br}\right\} + \frac{1}{2}\right] \tag{21}$$

In the above expression, the special function 'LambertW' with a general argument 'K' can be evaluated using the simplified expression given in Eq. (22).

$$\text{LambertW}\{K\} \approx \begin{cases} 0.665\{1 + 0.0195\ln(K+1)\}\ln(K+1) \\ \quad + 0.04, \quad 0 \leqslant K \leqslant 500 \\ \ln(K-4) - \{1 - 1/\ln(K)\}\ln\{\ln(K)\}, \\ \quad K > 500 \end{cases} \tag{22}$$

Entropy generation number (N_{ST}) is plotted as a function of radial distance in Fig. 4 for $\Pi = 2.0$, $\lambda = 0$, $Br = 1.0$, and for group parameters (Br/Ω) ranging 0 to 1. The group parameter determines the relative importance of viscous effects and has significant effect on entropy generation. For all group parameters, the inner cylinder acts as a strong concentrator of irreversibility. Entropy generation number is high in magnitude near the inner cylinder due to the high gradient of temperature and velocity. N_{ST} then falls exponential like along the radial direction and approaches an asymptote near the outer cylinder. N_{ST} profiles are similar in shape and almost parallel to one another whatever the value of group parameter, but vary in magnitudes. For constant Br, Π, and λ, the magnitude of N_{ST} depends only on the group parameter (Br/Ω) which is a part of the fluid friction irreversibility (N_F) term in entropy generation number (see Eq. (14)). So, an increasing or decreasing Br/Ω just increases or decreases the magnitude of the N_{ST} profile without changing its shape. At a particular radial position, magnitude of N_{ST} is higher for higher group parameter.

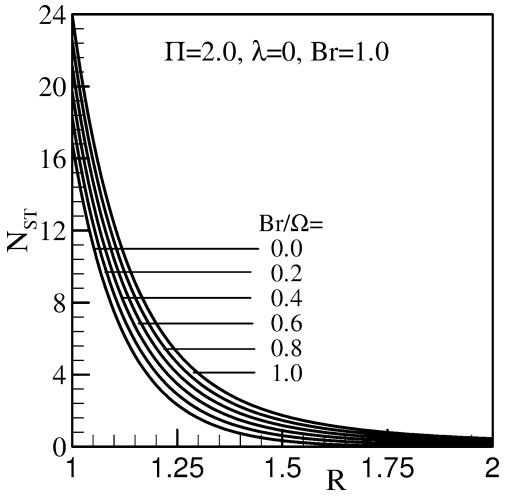

Fig. 4. Isothermal entropy generation profiles at different group parameters.

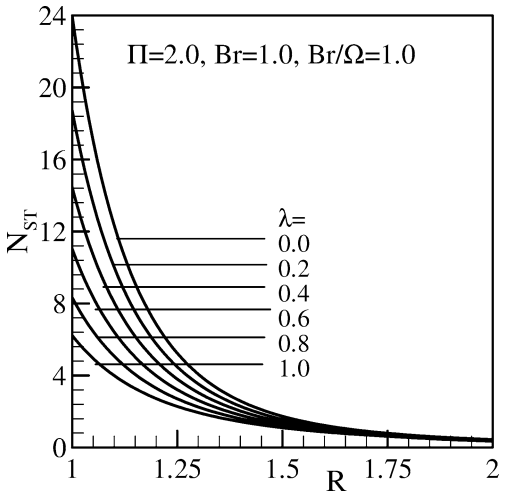

Fig. 5. Isothermal entropy generation profiles at different velocity ratios.

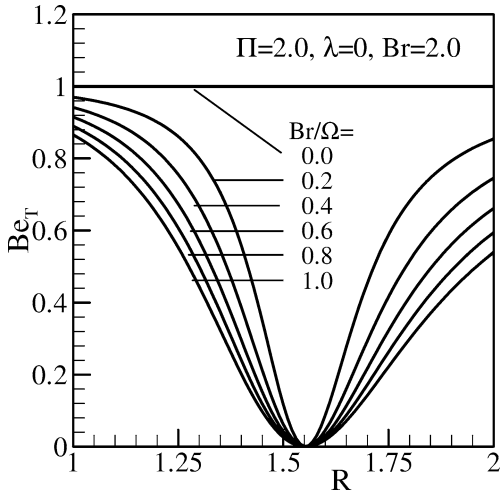

Fig. 6. Isothermal Bejan number distribution at different group parameters.

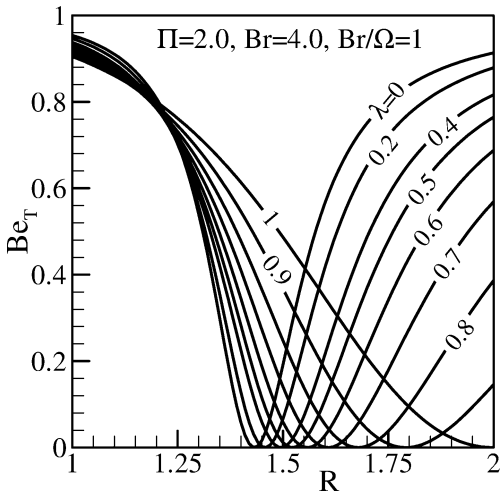

Fig. 7. Isothermal Bejan number distribution at different velocity ratios.

The effect of velocity ratio (λ) on entropy generation is presented in Fig. 5 for $\Pi = 2.0$, $Br = 1.0$ and $Br/\Omega = 1.0$. Value of λ is kept between 0 and 1 because of practical importance. The inner wall still acts as a strong concentrator of irreversibility, but now the magnitude of N_{ST} drops significantly at the inner wall for higher λ due to the lower temperature and velocity gradients. With the increase of radial distance, N_{ST} profiles approaches one another and merge at or near $R = 1.70$. N_{ST} is inversely proportional to the R, R^2, R^3 terms (see Eq. (14)). For constant Br, Br/Ω, and λ, N_{ST} falls with increasing R. It is interesting to note that a big contribution to entropy generation comes from the first of the three parts inside the first square bracketed term (N_R) of Eq. (14). When R approaches Π, the first one of these three parts approaches zero. Initially (at low R) N_{ST} shows different magnitude for different λ, but with the increasing R contribution to the entropy generation from the dominating term decreases resulting a trends of merging profiles with each other. The magnitude of entropy generation number is same for rest of the radial distance.

Bejan number (Be_T) is plotted in Fig. 6 as a function of radial distance for $\Pi = 2.0$, $\lambda = 0$, $Br = 2.0$, and group parameters 0 to 1. For $Br/\Omega = 0$, fluid friction contribution to entropy generation is zero. The Bejan number is equal to its maximum value (= 1) and independent of radial distance at this group parameter. For $Br/\Omega > 0$, Be_T is still maximum at the inner wall, but its magnitude drops with the increase of Br/Ω. With the increase of radial distance, Be_T falls and approaches zero at $R \approx 1.55$ for all values of group parameters. The zero value of Be_T is due to the maximum radial temperature gradient at this point and this location can be determined by Eqs. (21) and (22).

The effect of velocity ratio λ on Be_T is shown in Fig. 7 where Be_T is plotted against R for $\Pi = 2.0$, $Br = 4.0$, and $Br/\Omega = 1$. Heat transfer irreversibility is still maximum at the inner wall for all values of λ due to high temperature and velocity gradient. The magnitude of Be_T is higher for lower value of λ at the inner wall. Be_T then falls along the radial direction. For all values of λ, profiles of Be_T intersect with one another at $R \approx 1.2$. Contribution of heat

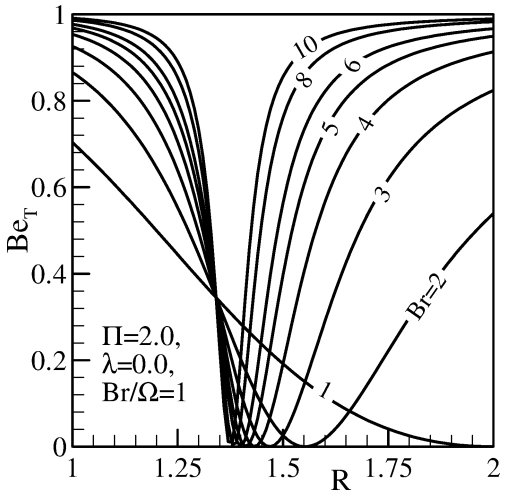

Fig. 8. Isothermal Bejan number distribution at different Brinkman numbers.

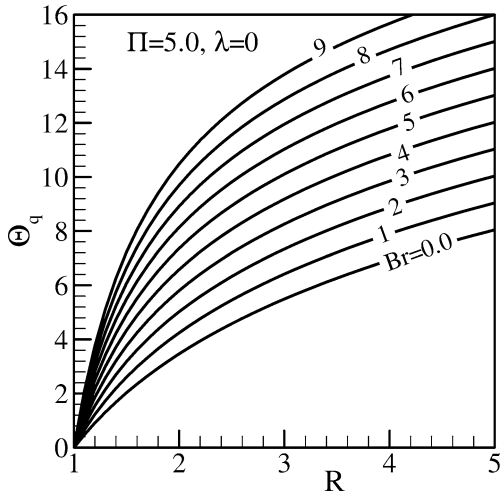

Fig. 9. Temperature distribution for the isoflux boundary condition.

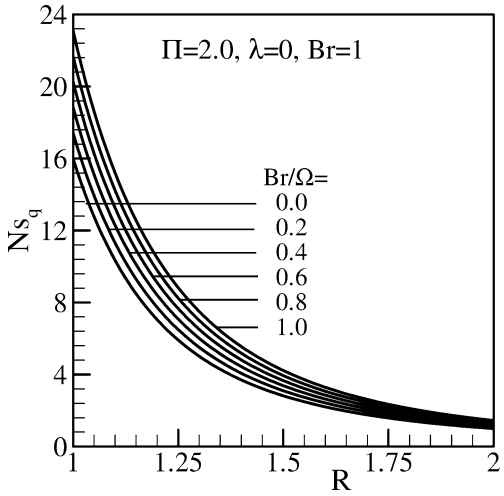

Fig. 10. Isoflux entropy generation profiles at different group parameters.

transfer irreversibility to entropy generation is the same at this point for all velocity ratios (λ) provided that $\lambda \leqslant 1$. This behavior depends on the Brinkman number as long as the radius ratio (Π) is kept constant. The lowest location of Be_T profile, which represents the zero contribution of heat transfer irreversibility, shifts towards the outer cylinder for higher λ. In Fig. 8, the effect of the Brinkman number on heat transfer irreversibility is presented for $\Pi = 2.0$, $\lambda = 0$, $Br/\Omega = 1.0$. For $Br = 1$, the Bejan number falls along the radial direction and no distinct minimum point is observed inside the annular gap due to the absence of any peak in temperature distribution. For $Br > 1$, the Bejan number falls rapidly along the radial direction, touches the minimum value ($= 0$) and then increases towards the outer cylinder. The minimum location for Be_T profile shifts towards the outer cylinder for lower Br. Be_T is higher at the higher value of Br at both the inner and outer cylinders.

For the isoflux boundary condition, dimensionless temperature profiles are plotted as a function of radial distance in Fig. 9 for different Brinkman numbers. Temperature profiles in this case are not similar in shape to the isothermal case. The temperature gradient is higher near the inner cylinder and this gradient increases with Br. Temperature increases along the radial direction with the decreasing radial temperature gradient. Temperature gradient is inversely proportional to R (see Eq. (10)). So, with increasing R, slope of the $\Theta_q - R$ profile decreases. For a particular radial position, temperature is higher for higher value of Br. Fig. 10 shows the variation of entropy generation number (N_{Sq}) with radial distance for $\Pi = 2.0$, $\lambda = 0$, and $Br = 1.0$ at different group parameters. The magnitudes of entropy generation numbers for both isothermal and isoflux cases are very much comparable though the temperature is higher for isoflux boundary condition. Because the basic equation (Eq. (13)) which is used for generating expression for entropy generation number deals with gradient of temperature instead of the magnitude of temperature. N_{Sq} profiles are very much similar to N_{ST} profiles except the slower falling rate that is observed for the isoflux boundary condition. The effect of velocity ratio on entropy generation is presented in Fig. 11 and the profiles are very much similar to the isothermal case.

The dimensionless volumetric averaged entropy generation rate (N^o_{ST}) can be evaluated using Eq. (23) for the isothermal case

$$N^o_{ST} = \frac{1}{\forall}\int_{\forall} N_{ST}\,\mathrm{d}\forall = \frac{1}{\forall}\int_{\forall} N_{ST} r\,\mathrm{d}\theta\,\mathrm{d}r\,\mathrm{d}z = f(Br, Br/\Omega, \Pi, \lambda) \tag{23}$$

In the above equation, $\forall$ is the volume of the annular space. Average entropy generation rate is a function of geometric parameter Π, flow parameter λ, dimensionless numbers Br, and group parameter Br/Ω. For a significant practical interest, we focus our attention on parameters Π and λ. Fig. 12 shows the distribution of average entropy generation as function of velocity ratio for $\Pi = 2.0$ and $Br = 2.0$ at different group parameter. Velocity ratio (λ) is kept between -1 to 5 for convenience. Both cylinders rotate

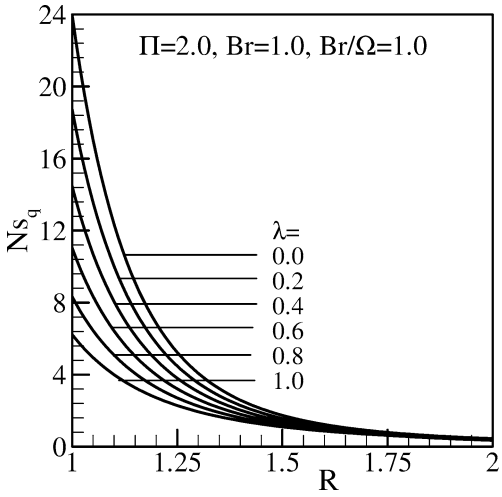

Fig. 11. Isoflux entropy generation profiles at different velocity ratios.

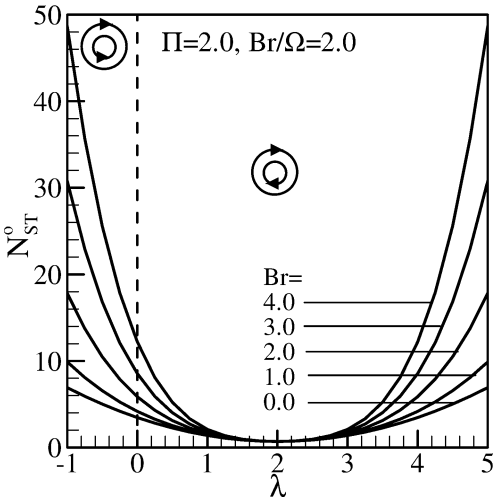

Fig. 13. Average entropy generation profiles at different Brinkman numbers.

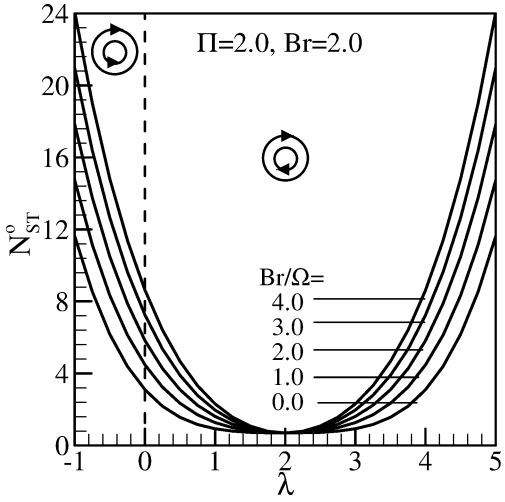

Fig. 12. Average entropy generation profiles at different group parameters.

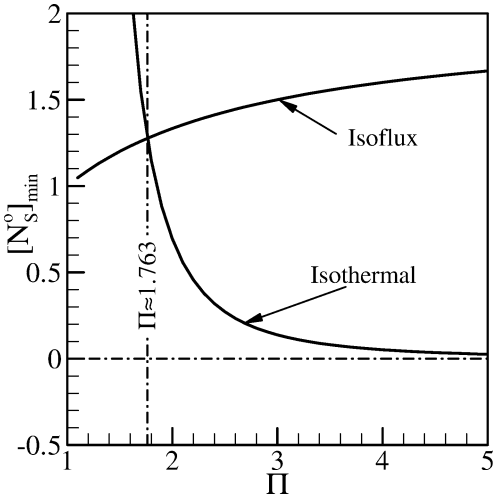

Fig. 14. Minimum average entropy generation profiles.

in same direction for positive λ and opposite directions for negative λ. The dashed line represents the Couette flow situation where $\lambda = 0$ (fixed outer cylinder). For this range of λ, average entropy generation rate (N^o_{ST}) shows a concave shaped distribution pattern. For all group parameters, the magnitude of minimum N^o_{ST} is same (≈ 0.6937) and which occurs at $\lambda = 2.0$. Except $\lambda = 2.0$, N^o_{ST} is higher for higher group parameter. N^o_{ST} is plotted against λ at different Brinkman numbers in Fig. 13. A similar concave shaped pattern is observed and each *Br*, profile is symmetrical about the $\lambda = 2.0$ line. For all values of *Br*, minimum N^o_{ST} is the same and equal to 0.6937. Except $\lambda = 2.0$, magnitude of N^o_{ST} is higher for higher *Br*. To locate the minimum N^o_{ST}, Eq. (23) is differentiated with respect to λ resulting a third order polynomial as follows

$$\frac{\partial N^o_{ST}}{\partial \lambda} = 0 = f_\lambda(Br, Br/\Omega, \Pi, \lambda) = K_0 + K_1\lambda + K_2\lambda^2 + K_3\lambda^3 \quad (24)$$

where K_0–K_3 are coefficients at different power of λ and function of *Br*, Br/Ω, and Π. Eq. (24) has three solutions and two of them give imaginary results. The only real solution is $\lambda = \Pi$. Fortunately, prior graphical presentations (Figs. 12 and 13) satisfy this solution ($\lambda = \Pi$) for minimum N^o_{ST}. For $\lambda = \Pi$, the angular velocity of the outer cylinder (ω_1) is equal to the inner cylinder (ω_0), i.e., no relative angular motion exists between the outer and inner cylinders. After substituting $\lambda = \Pi$ in Eq. (23), the expression for minimum N^o_{ST} becomes

$$\left[N^o_{ST}\right]_{\min} = \frac{2}{\Pi(\Pi+1)[\ln(\Pi)]^2} \quad (25)$$

$[N^o_{ST}]_{\min}$ is only a function of geometric parameter Π and independent of *Br*, Br/Ω. This can be easily verified from Figs. 12 and 13 where for all values of the group parameter and the Brinkman number, the magnitude of minimum entropy generation is same. A similar scenario is observed for the isoflux boundary condition except for the magnitude

of minimum average entropy generation rate ($[N^o_{Sq}]_{\min}$). $[N^o_{Sq}]_{\min}$ can be calculated using the following equation

$$\left[N^o_{Sq}\right]_{\min} = \frac{2\Pi}{\Pi + 1} \tag{26}$$

Fig. 14 shows the combined distributions of $[N^o_{ST}]_{\min}$ and $[N^o_{Sq}]_{\min}$ with radius ratio Π. At the two extremes, $\Pi \to 1$ and $\Pi \to \infty$, $[N^o_{ST}]_{\min}$ shows an asymptotic nature. In contrast, $[N^o_{Sq}]_{\min}$ shows an asymptotic nature only when $\Pi \to \infty$. At $\Pi = 1.763$, minimum entropy generation for both boundary conditions are equal at 1.2761. At the upper extreme of Π ($\Pi \to \infty$), minimum entropy generation rate approaches 0 for the isothermal case and 2 for the isoflux case.

4. Conclusions

The First and Second Laws of Thermodynamics are applied to forced convection inside a cylindrical annular space with both isothermal and isoflux boundary conditions to obtain general expressions for velocity and temperature distribution, entropy generation number, and Bejan number. Flow inside the annular gap is induced by the relative rotating motion between the inner and the outer cylinders. Near the inner cylinder, the entropy generation rate is higher due to the higher temperature and velocity gradients. The entropy generation rate shows asymptotic behavior near the outer cylinder provided that the rotation of the inner cylinder is higher than the outer. For different group parameters, N_S profiles are nearly parallel to one another. Difference between the magnitudes of two consecutive N_S decreases very slowly along the radial distance. Velocity ratio affects entropy generation number significantly. Difference between the magnitude of two consecutive N_S decreases rapidly along the radial direction and approaches zero near the outer cylinder. For the isothermal boundary condition, the Bejan number is maximum at the inner cylinder. The Bejan number decreases along the radial direction showing a minimum and then increase towards the outer cylinder as long as $Br/\Omega > 0$. The magnitude of the Bejan number is zero at its minimum location which can be determined by using the expression given in Eq. (21). The minimum value of average entropy generation rate depends only on radius ratio and it occurs when numerical value of λ is equal to the numerical value of Π.

Acknowledgements

One of the authors (Shohel Mahmud) wishes to thank 'The Canadian Commonwealth Scholarship Program of the Canadian Department of Foreign Affairs and International Trade' for the scholarship and the financial support to conduct the present research.

References

[1] D.M. Maron, S. Cohen, Hydrodynamics and heat/mass transfer near rotating surfaces, Adv. Heat Transfer 21 (1991) 141–183.
[2] G.I. Taylor, Distribution of velocity and temperature between concentric rotating cylinders, Proc. Roy Soc. London Ser. A 151 (1935) 494–512.
[3] K.N. Astill, Studies of the developing flow between concentric cylinders with the inner cylinder rotating, J. Heat Transfer 86 (1964) 383–392.
[4] C.D. Andereck, S.S. Lui, H.L. Swinney, Flow regimes in a circular Couette systems with independently rotating cylinder, J. Fluid Mech. 164 (1983) 155–183.
[5] I.S. Bjorklund, W.H. Kaye, Heat transfer between concentric rotating cylinders, J. Heat Transfer 81 (1959) 175–186.
[6] F. Tachibana, S. Fukui, H. Mitsumura, Heat transfer in an annulus with an inner rotating cylinder, Bull. JSME 8 (1960) 119–123.
[7] H. Aoki, H. Nohira, H. Arai, Convective heat transfer in an annulus with an inner rotating cylinder, Bull. JSME 10 (1967) 523–532.
[8] E. Leonardi, J.A. Reizes, G. de Vahl Davis, Heat transfer in a vertical rotating annulus—a numerical study, in: Proc. 7th Internat. Heat transfer Conf., Munich, 1982.
[9] M.A. El-Shaarawi, A. Sarhan, Developing laminar free convection in an open ended vertical annulus with a rotating inner cylinder, J. Fluid Mech. 102 (1983) 552–558.
[10] S.R.M. Gardiner, R.H. Sabersky, Heat transfer in an annular gap, Internat. J. Heat Mass Transfer 21 (1978) 1459–1466.
[11] C.J.R. Gasley, Heat transfer characteristics of the rotating and an axial flow between concentric cylinders, J. Heat Transfer 80 (1958) 79–90.
[12] L.A. Dorfman, Heat and mass transfer near rotating surfaces, J. Engrg. Phys. 22 (1972) 247–257.
[13] P.R.N. Childs, C.A. Long, Review of forced convective heat transfer in stationary and rotating annuli, J. Mech. Engrg. Sci. 210 (1996) 123–134.
[14] A. Bejan, Second-law analysis in heat transfer and thermal design, Adv. Heat Transfer 15 (1982) 1–58.
[15] A. Bejan, Entropy Generation Minimization, CRC, Boca Raton, NY, 1996.
[16] A. Bejan, A study of entropy generation in fundamental convective heat transfer, J. Heat Transfer 101 (1979) 718–725.
[17] B.S. Yilbas, Entropy analysis of concentric annuli with rotating outer cylinder, Exergy Internat. J. 1 (2001) 60–66.
[18] M.K. Drost, J.R. Zaworski, A review of second law analysis techniques applicable to basic thermal science research, ASME AES 4 (1988) 7–12.
[19] F.M. White, Viscous Fluid Flow, McGraw-Hill, New York, 1974.
[20] S. Paoletti, F. Rispoli, E. Sciubba, Calculation of exergetic losses in compact heat exchanger passages, ASME AES 10 (1989) 21–29.
[21] A. Bejan, Shape and Structure, from Engineering to Nature, Cambridge University Press, Cambridge, 2000.
[22] L.G. Leal, Laminar Flow and Convective Transport Process: Scaling Principles and Asymptotic Analysis, Butterworth–Heinemann, Stoneham, 1992.